Numerical simulation of fluid flow, solidification and defects in high pressure die casting (HPDC) process

IOP Conf. Series: Materials Science and Engineering **529** (2019) 012058 doi:10.1088/1757-899X/529/1/012058

Numerical simulation of fluid flow, solidification and defects in high pressure die casting (HPDC) process

K Dou[1], E Lordan[1], Y J Zhang[1], A Jacot[1] and Z Y Fan[1]

[1] Brunel Centre for Advanced Solidification Technology (BCAST), Brunel University London, Kingston Lane, Uxbridge, UB8 3PH, United Kingdom

E-mail: Kun.Dou@brunel.ac.uk

Abstract. The high pressure die casting process is extensively used to manufacture light metal parts with high productivity. A major drawback of the process is the relatively high variability in mechanical properties and poor repeatability between casting cycles, limiting the achievement of weight reduction through lighter design. Although it has been established that mechanical properties are adversely affected by casting defects, the origin of the relatively high randomness in the HPDC process is not well understood. Numerical simulation is a powerful and cost-effective tool to address this question, as it gives access to quantities that are difficult to obtain experimentally. A numerical simulation approach based on the finite element casting software ProCAST has been developed. The model was applied to the casting of aluminium tensile test samples, which were used to measure the tensile properties of the alloy. Simulation permitted the study of fluid flow, solidification and defect formation during each stage of the HPDC process: pouring, injection and cooling. Air entrapment and porosity distribution in the cast part were predicted. The results were compared with temperature measurements, porosity observations and solid distribution in the sleeve prior to injection. Although the results are still very preliminary, some trends could be established between the level of turbulence of the melt during injection and reduced elongation.

1. Introduction

The high pressure die casting process (HPDC) is widely used within the automotive industry to produce parts requiring high dimensional accuracy and low surface roughness, exhibiting great productivity and competitive cost for mass production [1,2]. The application of light metal castings manufactured by HPDC is an effective way to reduce vehicle weight and limit carbon emissions. HPDC products exhibit good mechanical properties due to fine grain formation under rapid cooling. However, some variability in mechanical properties among different positions in the die and batches is often observed[3-5]. Although it has been established that mechanical properties are adversely affected by casting defects[6], the origin of the relatively high randomness in the HPDC process is not well understood. Optimizing the mechanical properties and controlling their variability through trial-and-error experiments can prove to be time-consuming and it is likely that the procedure will have to be repeated for new designs. More fundamental understanding is thus desired to be better guided in this procedure. A combined approach based on both experiments and simulation was developed to address the topic. The present contribution is focused on the modelling effort to bring insight on fluid flow, solidification and defect formation

during each stage of the HPDC process, including the role of the sample position in the die. The results are compared with experimental data and the possible origin of the variability of the mechanical properties is analysed.

2. Experimental

Silafont-36 (Al-9Si-0.3Mg-0.5Mn) was used throughout this work. A 40 Kg crucible of Silafont-36 was melted in an electric resistance furnaces and held at 750°C for 30 min to maintain a uniform composition distribution. Then, the melt was degassed using the HSMC device[7]. This process involved two phases (i) degassing for 10 min at a rotor speed of 1500 rpm and an argon flow rate of 0.2 L/min, followed by (ii) conditioning via intensive melt shearing for an additional 20 min without argon flow. Following melt treatment, molten metal was poured into the shot sleeve of a Bühler 4500 kN locking force cold chamber HPDC machine using a transfer ladle. The temperature of the melt, shot sleeve and die cavity were maintained at 680°C, 180°C and 150°C respectively. The molten metal was then injected into the die cavity at a slow shot speed of 0.3 ms-1 and a filling speed of 3.6 ms-1 to produce eight round tensile samples with a nominal gauge diameter of ø6.35 mm in accordance with ASTM standards. The geometry of the samples and gating system is illustrated in Figure 1.

3. Modelling

As HPDC is a complex process involving high thermal gradients, high fluid velocities, and high probability for the melt free surface to fold and fragment, it is important to address all the stages of the process, starting with shot sleeve filling, followed by melt injection (using the actual piston kinematics), and finally solidification inside the die. The commercial casting simulation suite ProCAST was used to simulate the whole process. The CAD models for the casting volume, the shot sleeve, the fixed/mobile dies and the shot piston were built and assembled in VisualMesh[11]. A finite element (FE) mesh was then generated accordingly with a minimum mesh size of 0.5 mm to ensure an accurate description of fluid flow through the thin ingate (2 mm×5 mm). Details about the geometry and meshes are shown in Figure 1. Fluid flow, heat transfer and solidification of the melt during the different steps of the process were modelled with the ProCAST solver, which calculates the evolution of the melt free surface with a Volume of Fluid (VOF) method and solves coupled conservation equations of momentum, mass, and heat [8-10].

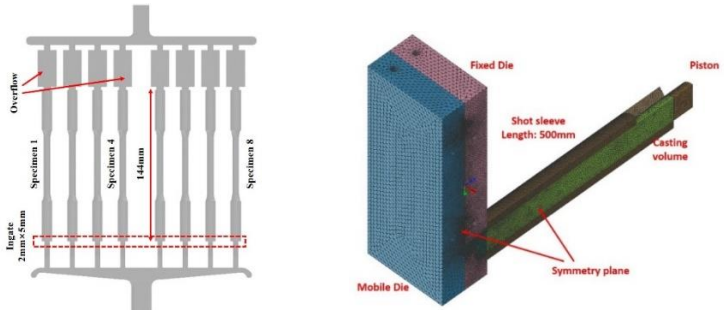

Figure 1 Geometry of the casting and gating system (left) and finite element mesh used for the simulation (right).

(left: tensile sample casting in full symmetry, right: HPDC configuration in half symmetry with FE meshes)

The Al melt was treated as an incompressible fluid. The amount of entrained air in the melt and final casting was predicted qualitatively using the *GAS* model[11,12], which is based on a prediction of the turbulence/fragmentation of the free surface. In addition, the *Advanced Porosity Module* (APM)[13-15] was also used to solve the Darcy equation and the segregation of gas in the mushy zone, in order to predict the distribution of microporosity in samples.

3.1 Simulation conditions

The pouring of the melt through the pouring hole in the shot sleeve was simulated with an inlet boundary condition, which specifies the amount of metal flowing through a selected surface section. In the HPDC process, the inner wall of the shot sleeve is typically coated with oil for protection and lubrication, which can influence the flow and heat transfer at the interface. In this work, a temperature dependent interfacial heat transfer coefficient (iHTC) and a dedicated function to account for the effect of the surface roughness on the boundary layer at the wall (*WALLF function*[11]) were used to account for these effects. The piston movement during the shot sleeve injection process was defined based on the displacement curves obtained from the HPDC machine control panel. To better simulate the intensification stage of the HPDC process, a critical solid fraction of 0.95 was assumed as a threshold under which the biscuit region can still be fed with melt continuously.

3.2 Model validation

Dedicated experiments were carried out to validate the heat transfer analysis and the solid distribution predicted by the model. The melt temperature at different locations in the shot sleeve was measured with thermocouples and the distribution of the solid was analysed by emptying the content of the shot sleeve instead of proceeding with injection. As can be seen in Figure 2 (left), the predicted and measured temperatures are in good agreement. The main discrepancies are observed when the thermocouples are reached by the melt, which is explained by their relatively high response time (~1 s). In addition, it is observed that the shape of the metal after partial solidification in the sleeve closely resemble those predicted (Figure 2, right).

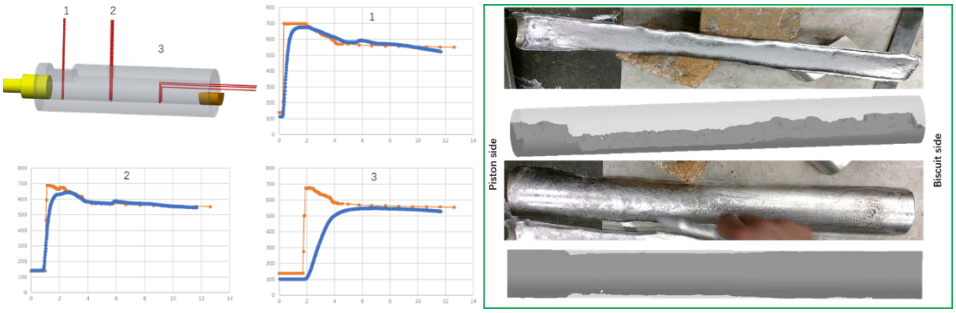

Figure 2 Comparison of temperature prediction (left) and solid shape (right) in the shot sleeve.

4. Results and Discussions

4.1 Pre-solidification in the shot sleeve

When the melt is poured into the shot sleeve, the contact with the relatively cold piston and shot sleeve leads to the formation of solid, which is usually referred to as externally solidified crystals (ESCs). Although the solid crystals were not directly modelled in this approach, solid formation in the sleeve could be predicted. Figure 3 shows the evolution of the solid fraction prior to melt injection. It could be seen that solid forms near the piston and at the bottom of the sleeve due to rapid cooling. As the melt front progresses towards the biscuit, more solid forms at the bottom of the shot sleeve. During the slow injection stage, the solid in contact with the piston is pushed with the potential for some crystals to re-melt. During the fast injection stage, the mixture is transported at high velocity into the die cavity and subsequently solidifies.

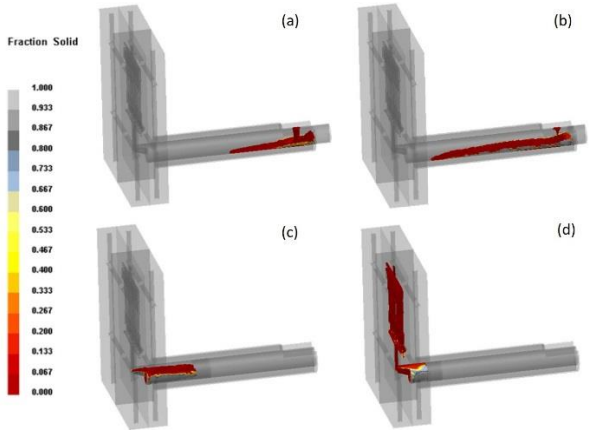

Figure 3 Evolution of the solid fraction in the shot sleeve, gating system and die during injection.

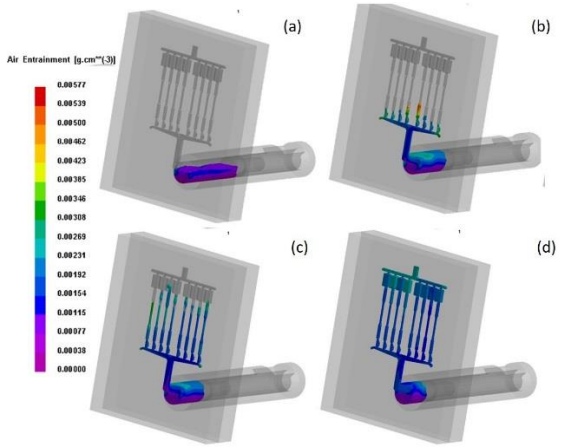

Figure 4 Predicted air entrainment during filling and injection.

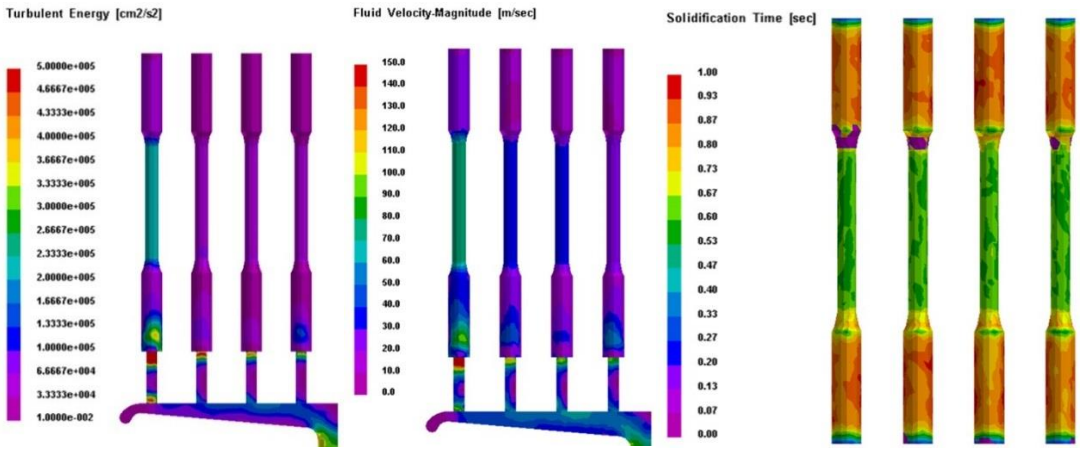

Figure 5 Calculated turbulence energy, melt velocity and solidification time in the tensile bars.

4.2 Air entrainment

Figure 4 illustrates the predicted evolution of entrained air during the process. As the plunger accelerates during the first stage, the melt is pushed towards the biscuit. Most of the air in the shot sleeve is driven out, but some can be entrapped at the melt front, the amount being largely determined by the shape of the wave. During the second stage, the melt is injected into the die at high speed. A certain amount of air accumulates and is trapped inside the final casting. Optimizing the design of venting systems, the motion of the plunger and the application of vacuum devices can minimize the amount of entrapped air, which is beyond the scope of the present study.

4.3 Fluid flow and solidification in die cavity

As shown in Figure 5, during the die filling process, vigorous turbulences are predicted at the ingate sections, which leading to substantial differences in turbulent energy and maximum velocity inside the tensile sample cavities. It can be seen that the maximum velocity magnitude exceeds 100 m/s at the ingate area. The fluid velocity magnitude reaches about 80 ms-1 in the left cavity however does not exceed 20 ms-1 in the right one. Such differences in fluid velocity magnitude can potentially influence the variability of properties between cast parts for a given shot.

4.4 Porosity

Porosity defects in casting can be categorized into macro- and micro-porosities based on their sizes[17-19]. Microporosities can themselves be categorized into gas and shrinkage porosity based on their morphology. In this paper, two distinct models were used to assess porosity: the standard POROS model of ProCAST[11, 12], which focuses on shrinkage and macro porosity, and the advanced porosity model (APM) [14] , which addresses different categories of porosity. Optical microscopy was carried out on the tensile test samples to characterize porosity. Figure 6 (left) shows that the POROS model correctly predicts the formation of a large amount of porosity at the bottom of the bars, due to feeding difficulties. The rather spherical shape indicates that gas certainly played an important role in the formation of the pores. The APM model predicts the presence of microporosities only in the thicker ends of the bar, which is confirmed by the observation (Figure 6, right).

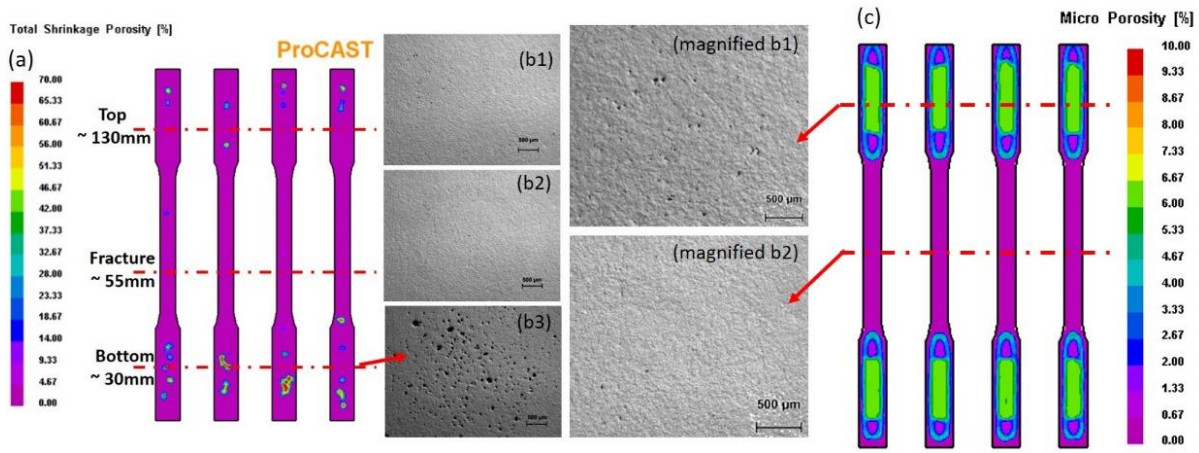

Figure 6 porosity distribution in the tensile samples (modelling and experiments)

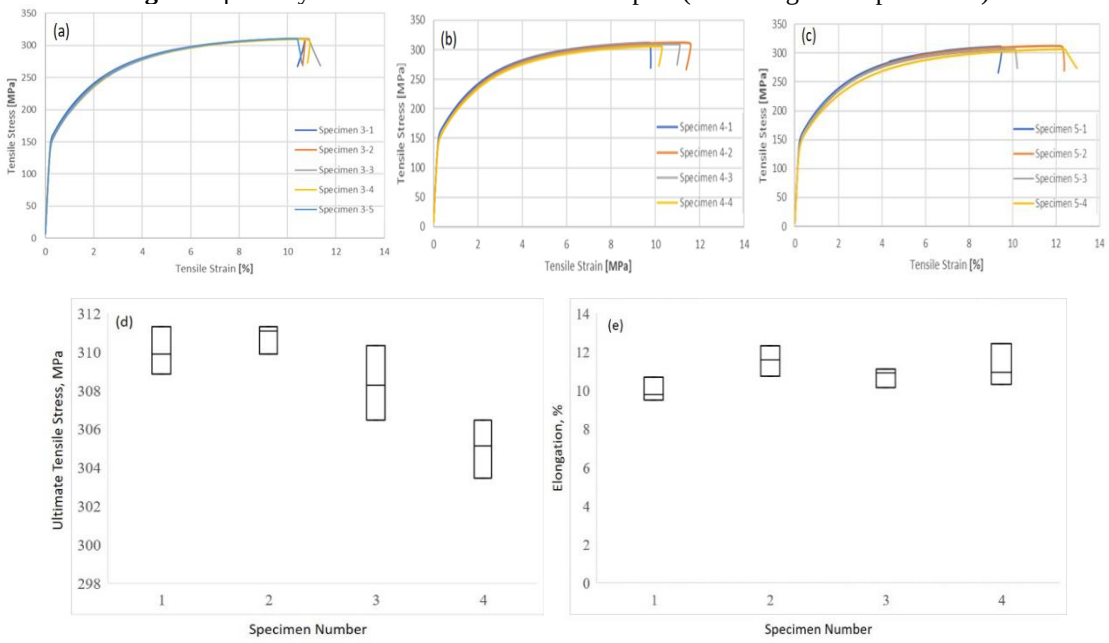

Figure 7 Test results for tensile stress and elongation of samples in different locations

4.5 Mechanical properties

The tensile properties of samples from three consecutive shots are shown in Figure 7a, 7b and 7c for

different positions in the die (See Figure 1 for the position labels). Scatter plots of the ultimate tensile stress and elongation as a function of position are presented in Figure 7c and 7d (Refer to Figure 1 for the position labels). It can be observed that elongation exhibits higher relative variations than UTS and that, globally, the position in the die does not seem to play an obvious influence on the properties considering the data scatter. However, a tendency for reduced elongation at position #1 can be pointed out. According to the simulation, the highest level of turbulence and maximum melt velocities are obtained at position #1, which might be at the origin of this tendency. However more data is required to confirm this correlation.

5. Conclusion

A simulation approach has been developed to gain insight into melt flow, solidification and defect formation during the high pressure die casting of aluminium alloys. The evolution of the solid formed in the shot sleeve was analysed and discussed. Predictions of porosity showed to be in good agreement with empirical measurements. The UTS and elongation of the 12 tensile samples were measured. A trend for reduced elongation where the level of turbulence and melt velocities are the highest could be detected. More tensile data and further investigation is however required before the origin of variability in mechanical properties can be evidenced.

References

[1] Bonollo F, Gramegna N and Timelli G 2015 *JOM* **67** 901.
[2] Mordike B L and Tü Ebert 2001 *Mater. Sci. Eng. A* **302** 37.
[3] Lee S G, Patel G R, Gokhale A M, Sreeranganathan A and Horstemeyer M F 2006 *Mater. Sci. Eng. A* **427** 255.
[4] Gunasegaram D R, Finnin B R and Polivka F B 2007 *Mater. Sci. Tech.* **23** 847.
[5] Chen Z W 2003 *Mater. Sci. Eng. A* **348** 145.
[6] Ji S, Yang W, Jiang B, Patel JB, Fan Z 2013 *Mat. Sci. and Eng. A* **566** 119.
[7] Zhang Y J, Patel J B, Lazaro-Nebreda J and Fan Z Y 2018 *JOM* **70** 2726.
[8] Vijayaram T R, Sulaiman S, Hamouda A M and Ahmad M H 2006 *J. Mater. Proc. Tech.* **178** 29.
[9] Cleary P W, Ha J, Prakash M and Nguyen T 2010 *Appl. Math. Model.* **34** 2018.
[10] Guo J Z and Samonds M 2011 *JOM* **63** 19.
[11] ProCAST version 2018.1 User Manual 2018 ESI Group France.
[12] Guo J Z, Makinde A and Bewlay B 2009 *Modeling of Casting Welding and Advanced Solidification Processes* (TMS: Warrendale) pp 337–344.
[13] Pequet C, Rappaz M and Gremaud M 2002 *Metall. Mater. Trans. A* **33** 2095.
[14] Guo J Z et al. 2015 *IOP Conference Series: Materials Science and Engineering* **84** (IOP Publishing).
[15] Carlson K D and Beckermann C 2009 *Metall. Mater. Trans. A* **40** 163.
[16] Gaël C and Rappaz M 2006 *TMS Annual Meeting*. No. LSMX-ARTICLE-2008-003.
[17] Lu Y, Taheri F, Gharghouri M A and Han H P 2009 *J. Alloy. Compd.* **470** 202.
[18] Lee S G and Gokhale A M 2006 *Scripta Mater.* **55** 387.
[19] Fan Z Y et al. 2009 *Int. J. Cast Metal Res.* **22** 103.

Acknowledgements

This project is financially supported by EPSRC UK in the EPSRC Centre for Innovative Manufacturing in Liquid Metal Engineering (The EPSRC Centre—LiME).